

## Durham Research Online

---

### Deposited in DRO:

27 May 2021

### Version of attached file:

Accepted Version

### Peer-review status of attached file:

Peer-reviewed

### Citation for published item:

Gillespie, Paul A. and Holdsworth, R.E. and Long, D. and Williams, A. and Gutmanis, J.C. (2021) 'Introduction: geology of fractured reservoirs.', Journal of the Geological Society, 178 (2).

### Further information on publisher's website:

<https://doi.org/10.1144/jgs2020-197>

### Publisher's copyright statement:

### Additional information:

---

### Use policy

The full-text may be used and/or reproduced, and given to third parties in any format or medium, without prior permission or charge, for personal research or study, educational, or not-for-profit purposes provided that:

- a full bibliographic reference is made to the original source
- a [link](#) is made to the metadata record in DRO
- the full-text is not changed in any way

The full-text must not be sold in any format or medium without the formal permission of the copyright holders.

Please consult the [full DRO policy](#) for further details.

# Introduction: Geology of Fractured Reservoirs

P.A. Gillespie<sup>1</sup>, R.E. Holdsworth<sup>2</sup>, D. Long<sup>3</sup>, A. Williams<sup>1</sup> and J.C. Gutmanis<sup>4</sup>

<sup>1</sup> Equinor ASA, Forusbeen 50, 4035, Stavanger, Norway

<sup>2</sup> Department of Earth Sciences, Durham University, Durham DH1 3LE, UK

<sup>3</sup> 2 Bucklerburn Drive, Peterculter, Aberdeen AB140XJ, UK

<sup>4</sup> Independent (JG Geology), 4 Capella Court, 42 Woodlane, Falmouth, Cornwall TR114QZ, UK

## Abstract

The characterisation of fractured reservoirs and fractured geothermal resources requires a thorough understanding of the geological processes that are involved during fracturing and the host rock rheological properties. The presence or absence of mechanical layering within the rock and the mode of failure substantially control the organization and scaling of the fracture system; subsequent chemical alteration and mineralization can both increase or decrease porosity and permeability. An integration of this understanding using information from outcrop analogues, together with static and dynamic subsurface data, can improve our ability to predict the behaviour of fractured reservoirs across a range of scales.

## Keywords

Fractured reservoir, geothermal, mechanical stratigraphy, basement, carbonate

The exploration for and production of fractured reservoirs is a complex task that can prove very demanding for the geoscientist. The data available are derived largely from scattered wells that provide a far from complete picture of the fracture system that controls flow. A critical aspect of characterising fractured reservoirs is to understand the geological setting and evolution of the fracture system and the lithology of the matrix. Matrix lithology determines both the brittleness of the rocks and their susceptibility to chemical alteration, while the burial history underpins the diagenesis and pore-fluid history of the reservoir. Fracture diagenesis may affect the growth and development of fracture systems. The stress history, including tectonic events, determines the nature and development of the fracture system, whilst past geological processes during fracture filling (e.g. mineralization, fault rock development, sediment ingress) and present-day stress can significantly affect fracture permeability.

The publications in this volume describe how geological understanding is used in the characterisation of fractured hydrocarbon reservoirs and geothermal resources.

The term fracture is used generically here to mean any planar or curvilinear structural discontinuity. The term “naturally fractured reservoir” refers to reservoirs that have permeability and connectivity that is enhanced by the development of open natural fractures. Reservoirs that contain only tight fractures, such as most porous sandstone reservoirs, are not termed fractured, even if they are heavily faulted; similarly, reservoirs that can only be produced following stimulation by hydraulic fracturing are not considered as “naturally” fractured reservoirs.

A typical feature of fractured reservoirs is that the permeability calculated from well tests is significantly higher than the permeability measured from core plugs. This is because the core plug measurements record the permeability of the matrix, whereas the well tests measure the effective permeability which is essentially the sum of the matrix and fracture permeability. Fractures in the porous matrix enable the transfer of fluids from the matrix blocks into the fracture due to the large contact surface area of the fracture. This process is particularly effective where there is a large contrast between a relatively low-permeability matrix and high permeability fracture, such as in many North Sea chalk reservoirs. Understanding the scale of the dynamic connectivity is key for calibration of fracture permeability at single well-bore to multi-well and reservoir scale.

The porosity due to fractures is usually small (usually significantly less than 1% of the rock volume), but the effect of fractures on permeability can be huge. A 100 m thick porous layer with 10 mD permeability has the same flow capacity as a 0.2 mm wide open horizontal fracture in an impermeable layer (calculated from the Poiseuille equation for parallel plates, van Golf Racht 1982). Many highly impermeable lithologies, such as cemented sandstone or carbonate mudstone, are brittle and so tend to be strongly fractured. The presence of open fractures allows fluids to be produced from such otherwise tight reservoirs. The flow characteristics of reservoir fluids, be it oil, gas or water, can each be affected differently by the rock properties of the matrix and the fractures, including wettability, relative permeability and capillary pressure.

## Types of Fractured Reservoirs

Fractured reservoirs are typically classified according to the relative contribution of fractures and matrix to the reservoir porosity and permeability, such as the modified version of Nelson's (2001) classification below:

**Type I:** fractures provide the essential reservoir porosity ( $\phi$ ) and permeability ( $k$ )

**Type II:** fractures provide the essential  $k$ , matrix provides storage capacity ( $\phi$ )

**Type III:** fractures assist  $k$  in an already producible reservoir

**Type IV:** fractures provide no additional  $\phi$  or  $k$ , but create significant reservoir anisotropy (barriers)

This classification gives a first order indication of the production characteristics of the reservoir. Type I reservoirs are typically found in basement rocks and tight carbonates. In Type II reservoirs, hydrocarbons drain from the matrix blocks and into the permeable fracture system, from where they are produced. Type III reservoirs have adequate matrix permeability for production of fluids, in addition to permeable fractures. Type IV represents reservoirs in which the fractures are less permeable than matrix (i.e. they act as baffles or barriers) and are therefore not strictly fractured reservoirs in the sense used in the hydrocarbon industry.

In fractured reservoirs with low matrix porosity and permeability (Type I or II above), the recovery factor is sensitive to aquifer drive strength and optimization of flow rate: such reservoirs are easily damaged by excessive production rates. In fractured microporous reservoirs, such as chalk (Type II above), the recovery is affected by inherent rock and fluid properties such as matrix permeability, fluid viscosity, wettability and fracture density (Allan and Sun 2003).

Fractured hydrocarbon reservoirs can occur in a wide range of rock types, including carbonates, silicified rocks, tight sandstone (e.g. tight gas sands), volcanic rocks and crystalline basement (e.g. gneiss, granite). In a global database of 314 fractured oil and gas reservoirs (C&C Reservoirs, 2020), carbonate reservoirs comprised 72% of the sample, whereas basement reservoirs represented 8% of fractured reservoirs and volcanic reservoirs only 2% (Figure 1).

The tectonic settings that have produced fractured reservoirs are variable, but out of the same dataset, 50% of fractured reservoirs occur in traps that were developed during contractional deformation (in the foreland or fold-thrust belt). This is in part due to the large number of fractured carbonate fields that are located in the Zagros fold belt and the Rocky Mountains and their forelands.

## Carbonates

Carbonate reservoirs are highly variable, ranging from reservoirs in which the matrix provides little contribution to the storage of fluids (Type I) and those with such good matrix properties that fractures have little impact on overall permeability (Type III). The development of fractures in carbonates is related to the depositional facies and pore types that are present, as well as to the tectonic history. Carbonates are highly active chemically, which means that they are prone to rapid cementation and dissolution.

Many of the largest and most productive of the world's hydrocarbon reservoirs are fractured carbonate reservoirs, including the giant carbonate reservoirs of the Middle East (Daniel 1954). The more recently discovered Cretaceous lacustrine reservoirs offshore Brazil (commonly termed "Pre-Salt") are also influenced by fractures (e.g. Salomão et al. 2015) and have become a focus of exploration and production activity since 2006.

In this thematic collection of papers, the Shaikan field of Iraq is described, which is a Jurassic fractured carbonate reservoir (Gilchrist et al. **this volume**; Price et al. **this volume**) and the Halalatang oilfield of the Tarim basin, China which is of Ordovician age (Ukar et al. **this volume**).

### ***Crystalline basement***

Most fractured basement plays are associated with the development of up-faulted buried hill traps (Biddle & Wielchowsky 1994), usually in extensional tectonic settings: the reservoirs occur in the footwalls of major normal faults. Fractured granitic basement has proven to be highly productive in Vietnam (Cuong and Warren 2009, Nguyen et al. 2011) and in the Gulf of Suez (Salah and Alsharhan 1998, Younes et al. 1998). In both cases the granitic basement has suffered deep weathering, providing additional solution-enhanced porosity (P'an 1982). Commercially successful fractured basement fields are typified by long hydrocarbon columns, which helps to diminish the risk of water breakthrough. They are usually classified as Type I reservoirs, as the matrix permeability of crystalline basement rocks is normally very low.

Recent hydrocarbon discoveries in fractured basement of the UK and the Norwegian continental shelves have generated new interest in this play type. On the Norwegian continental shelf, the Rolvsnes horizontal appraisal well on the Utsira High proved oil in fractured and weathered granitic basement with flow rates of 7000 bopd (Trice et al. 2019). In the UK, a series of discoveries have been made in the Rona Ridge, West of Shetland, including the Lancaster field (Trice et al. 2019, Holdsworth et al. **this volume**). The host rock for the discoveries of the Rona Ridge is a Neoarchaean charnockitic basement, which is cut by deep fissures extending downwards from a regional unconformity that are filled with fluids, sediment and minerals (Holdsworth et al. **this volume**). The Lewisian complex in NW Scotland provides a good onshore analogue for the basement rocks of the Rona Ridge, and has been used to develop a conceptual understanding of the fracture system and to collect quantitative fracture data that cannot be acquired from the subsurface (McCaffrey et al. **this volume**).

### ***Volcanics***

Whilst hydrocarbon fields in volcanics are typically relatively small (e.g. Magara 2003), the discovery of the Qingshen gas field in northeastern China, which has over 100 billion cubic metres (3.5 trillion cubic feet) of gas reserves (Feng 2008), has shown that they can be large. This reservoir, hosted in Cretaceous rhyolite and tuff lithologies, developed in a rift setting. Gas yields are highest on palaeomorphological highs where both fractures and secondary porosity are well developed, forming buried hill traps.

### ***Geothermal resources***

The production of geothermal energy requires high geothermal gradients and conductive heat flux. These systems are usually associated with younger volcanics, occurring for example at plate boundaries, where magma conduits exist, or in zones of high hydrothermal activity (Barbier 1997). For example, the Southern Negros Geothermal field in west central Philippines, (Primaleaon et al. **this volume**) is associated with the Cuernos de Negros volcanic complex; similarly, the Taupo Volcanic Zone of New Zealand contains geothermal resources in volcanic rocks, crystalline plutonic rocks and metamorphosed greywacke (McNamara et al. 2017). The Geysers geothermal resource in California is hosted in fractured greywacke that is heated by an underlying felsite intrusion associated with the Pliocene-Holocene Clear Lake volcanic field (Sammis et al 1992; Darymple et al. 1999). The permeability of many geothermal systems, especially those in tight formations, depends on fracture permeability with little contribution from the matrix and as such, they are directly comparable to Type I fractured reservoirs. The thermal energy that is stored in the rock matrix is extracted by circulation of water through the fracture system.

Enhanced geothermal systems (EGS or “hot dry rock” geothermal energy) produce energy from deep crystalline rocks, by actively injecting water into wells to be heated and pumped back out. The water is injected under high pressure which expands existing rock fractures and enables the water to freely flow in and out. The lithology of EGS reservoirs is typically igneous; 80% of EGS reservoirs occur in granitic rocks (data from Lu 2018). The Soultz-sous-Forêts EGS project in France (Vidal and Genter 2018) is hosted in granitic rocks and overlying Triassic sedimentary rocks. Here it has been found that the natural fracture permeability is highest in fracture networks formed at the sediment-fracture interfaces, where a high degree of geothermal alteration has occurred (Schill et al. 2017). The United Downs Geothermal Power Project currently in development in Cornwall uses two wells drilled into a fault zone at a depth of 2.3 to 5.2 km in high heat flow early Permian granite (Cotton et al. 2020). In this case, water will be injected into a natural groundwater circulation system where temperatures are known to exceed 170°C.

### ***Characterisation of fractures***

A brief review is given below of the geological factors that control the occurrence and properties of natural fractures in reservoirs. While it is difficult to make generalisations without sacrificing accuracy, the aim here is to provide some broad guidance that can be applied to the exploration, modelling, appraisal and development of fractured reservoirs and geothermal resources.

### ***Organisation of fracturing***

208 Fractures can be classified kinematically, based on their mode of failure:

- 209 • **Opening mode fractures (joints)** are formed in conditions of tensile effective stress. They  
210 are typically bedding perpendicular, forming during uplift, near surface extension or  
211 folding. Opening mode fractures form perpendicular to the least compressive stress,  $\sigma_3$ .  
212 In the subsurface, opening mode fractures may be open or may be partially to wholly  
213 mineral- or sediment-filled.
- 214 • **Shear mode fractures (faults and shear fractures)**, which offset markers, are formed  
215 under elevated differential stress during tectonic events. Shear-mode fractures form  
216 conjugate arrays that intersect parallel to  $\sigma_2$  and have an acute bisector parallel to  $\sigma_1$   
217 (Anderson 1905, but see also Healy et al. 2015). Shear mode fractures display very  
218 variable hydraulic properties.
- 219 • **Closing mode fractures (stylolites and compaction bands)** are formed under compressive  
220 effective stress and low differential stress, perpendicular to  $\sigma_1$ . They are commonly  
221 formed during burial but may also be tectonically driven. Closing mode fractures are  
222 typically tighter than the surrounding matrix. However, if they are mechanically or  
223 chemically reactivated, they can become hydraulically conductive (Graham Wall et al.  
224 2006). Stylolites are typically formed during compaction of carbonates by localised  
225 pressure solution and have a characteristic wavy or saw-tooth appearance. Compaction  
226 bands are rarer and form only in high permeability grainy rocks, typically by a  
227 combination of porosity collapse, cataclasis and pressure solution (Fossen et al. 2011;  
228 Wennberg et al. 2013).

229 Under certain conditions, **hybrid fractures** may occur in which more than one mode of  
230 failure is operative. For instance, in near surface conditions normal faults may develop an  
231 opening mode component (Holdsworth et al. **this volume**).

232 The fracture classification described above is fundamental, and the different classes of  
233 fractures have differing geometry and scaling properties. However, it is not always  
234 straightforward to distinguish the kinematic origin of fractures from subsurface data, so a  
235 more pragmatic approach may be needed when describing the fractures from wells. In  
236 particular, it is difficult to distinguish between small shear-mode fractures with no clearly  
237 visible displacement and opening mode fractures. In practice, fractures in wells may be  
238 categorised as "**faults**" which have clear shear offset (or supporting evidence from  
239 biostratigraphy) and "**fractures**" which have no clear shear offset; the latter category may in  
240 reality include both opening mode and shear mode fractures. In many natural fracture  
241 systems, shear and opening mode fractures are closely interlinked (Kim et al. 2003) and  
242 understanding their kinematic relationship may be difficult from subsurface data. Closing mode  
243 fractures such as stylolites can usually be identified from borehole image or core data. Any  
244 fracture classification based on image logs should be calibrated against core data, where  
245 available, in order to determine the fracture kinematics and fill.

246  
247 The vertical extent of fractures exerts an important control on vertical effective permeability  
248 and capillary continuity. The vertical propagation of natural fractures is controlled by  
249 mechanical contrasts and by the stress in the mechanical units. Fractures which are  
250 contained within individual mechanical units are termed *stratabound*, while fractures that  
251 extend through many units are termed *non-stratabound* (Figures 2 - 4; Odling et al. 1999).

Non-stratabound joints tend to form in clusters (Gillespie et al. 1999; Gillespie et al. 2001) and clusters of sub-parallel joints are sometimes termed fracture corridors (De Keizer et al. 2007; Questiaux and Couples 2010; Laubach et al. 2018).

Stratabound joints tend to be regularly spaced and form a continuous organised network. In modelling, this kind of fracturing is referred to as background fracturing. Where jointing units are separated by non-jointing units (Figure 4), the stratabound joints typically have a spacing that is proportional to the thickness of the jointing unit (Huang and Angelier 1989; Narr and Suppe 1991; Gross et al. 1995), or alternatively the fractures may develop in a series of regularly spaced clusters (Gillespie et al. 1999; Philip et al. 2005). However, many sedimentary fractured reservoirs consist of a stack of jointing units that are not separated by non-jointing units. In this case the mechanical unit thickness is not well-defined and a hierarchy of joints may occur at different scales (Strijker et al. 2012; Laubach et al. 2018; Corradetti et al. 2018; Gutmanis et al. 2018).

The simple relationship described above, in which the spatial organization of the fractures is controlled by their vertical extent through the stratigraphy, is not the complete picture, as the degree of fracture cementation also plays a role. Detailed field and subsurface observations indicate that fractures that are uncemented tend to be regularly or randomly spaced, whereas fractures that are partially cemented are more likely to be clustered (Hooker et al. 2013; Li et al. 2019).

In order to quantify the fracturing in stratified rocks, the *fracture stratigraphy* should be described, i.e. the variation in fracture extent and occurrence within the different units (Corbett et al. 1987; Bertotti et al. 2007; Laubach et al. 2009; Morris et al. 2009; Zahm and Hennings 2009). The term fracture stratigraphy is sometimes conflated with *mechanical stratigraphy*, which describes the mechanical changes in rocks in relation to the stratigraphy (Laubach et al. 2009). Understanding the fracture stratigraphy and the mechanical stratigraphy and how they evolved is important for the correct placement and completion of wells and helps in the definition of flow units within the reservoir. Ductile layers or weak interfaces represent mechanical contrasts which tend to impede the vertical propagation of fractures. This mechanism is important in limiting vertical effective permeability in layered heterogeneous rocks. In stacked units of similar elastic properties, the principle parameters controlling vertical joint propagation are the frictional properties of the interface and the depth at time of deformation and since the friction is greater on deeper interfaces, non-stratabound fractures are more prone to occur at significant depth (Gillespie et al. 2001).

Mechanical contrasts can be seen in igneous intrusions of different types. Felsic igneous plutons are typically unstratified, and so clustered, or irregular non-stratabound joints develop (Segall and Pollard 1983; Bertrand et al. 2015). However, in layered igneous intrusions or in metamorphic rocks, stratification may influence the fracturing (e.g. Foster and Hudleston 1986). In volcanic sills and lava flows, polygonal jointing may occur due to stress built up during cooling, providing a very well-connected fracture network (Hetényi et al. 2012; Gudmundsson & Løtveit 2012; Walker et al. 2013). In the oil-producing sills of the Nequen Basin, Argentina, the open fractures are thought to be a combination of cooling joints and tectonically induced fractures (Witte et al. 2012).



Tectonic faults tend to be non-stratabound, unless they reach a ductile layer such as a mobile shale or an evaporite unit (Ferrill et al. 2014). Tectonic faults are clustered (Gillespie et al. 1993, Johri et al. 2014), and are often surrounded by diffuse zones of fracturing termed *damage zones* (Figure 5; Solum & Huisman 2017; Gutmanis et al. 2018, McCaffrey et al. **this volume** Figure 3f). Damage accumulates at asperities along the fault and at branch lines, relay zones and fault intersections (Rotevatn and Bastesen 2014; Nixon et al. 2019). Damage zones associated with faults that are large enough to cut through the entire reservoir can provide high permeability pathways that dominate fluid flow both vertically and horizontally (Paul et al. 2009).

### ***Conditions of fracture formation***

According to the principles of rock mechanics, opening mode and shear fractures develop under distinct stress conditions. Faults are formed under elevated differential stress, typically during tectonic events. Joints form under conditions of low differential stress (Price and Cosgrove 1990) and are therefore less likely to form during tectonic events, in which differential stress is high. Joint formation requires the effective stress be tensile, which can happen close to the surface or at elevated pore fluid pressure; joints can form during uplift as a result of thermal and elastic contraction (Engelder 1993). Care must be taken in using outcrop analogues of joint systems, as not all of the fracture sets observed at the surface may be present in the subsurface.

Gravitational collapse of caverns can cause extensive brecciation (Daniels et al. 2020), as can events of overpressure related to faulting (Sibson 1996) or volcanic processes. In breccias, the fractures may have components of both opening and shear mode.

In the subsurface it is important to analyse the wider, potentially basin-scale, depositional and tectonic history in order to reconstruct the framework of faulting and fracturing styles. Geologically heterogeneous sequences can lead to a large degree of local stress variation, resulting in many different fault and fracture types and fracture-intersection relationships, which can often only be deciphered at outcrop.

### ***Joint aperture and fill***

Opening-mode fractures create voids and the size of these voids are altered by chemical processes, namely precipitation and dissolution (Wennberg et al. 2016; Lima and De Ros 2019). In a chemically inactive system, such as may occur at shallow depths, joints have a mechanical aperture (opening) that is controlled by mechanical parameters alone. Under conditions of elevated pore fluid pressure, joints may be fully open, with an aperture controlled by the effective stress and the rock properties. At lower fluid pressures the walls of the fracture are partially in contact and the fracture aperture is defined by patches of the fracture that are not in contact, which reduce in area as the effective compressive stress increases (Pyrak-Nolte et al. 2000). In more chemically active systems, the aperture of the joint may become occluded by precipitating minerals (Laubach et al. 2004; Gale et al. 2010; Wennberg et al. 2016; Laubach et al. 2019), leading to a decrease in reservoir productivity (Laubach 2003). These are variously referred to as cemented, healed or sealed fractures (Anders et al. 2014 for review of the terminology).

## ***Fault properties***

Faults have highly variable lithological and mineralogical content, according to the mechanical properties of the host rock together with the fluid and stress history (see Bense et al. 2013 for review). In porous sandstone or grainstone, deformation within the damage zone is accommodated by compactional shear, leading to the formation of deformation bands (more precisely, shear bands), that have lower permeability than the host rock (Micarelli et al. 2006; Wennberg et al. 2013; Kaminskaite et al. 2019). More commonly, in rocks of low porosity (e.g. carbonate mudstone or crystalline basement), faults are accommodated by dilational shear, in which open fractures and an open fault breccia is developed, so that faults become hydraulically conductive (Crawford and Yale 2002). Experience from fractured reservoirs indicates that faults tend to be highly conductive, but they can also act as combined barriers and conduits (e.g. Caine et al. 1996; Agosta 2008).

The porosity in the fault zone may be occluded by precipitation of minerals (Woodcock et al 2007). Fault reactivation tends to cause breakage of mineral fills and re-opening of the fault; the faults that have most recently been active are those that are most likely to be open. In cases where open fractures are only partially filled, the fill can act as a natural prop counteracting the effects of in-situ stress loading and enhancing long-term permeability of a fractured reservoir (Holdsworth et al. 2019). Where there is shale in the faulted sequence, the shale may be smeared into the fault zone and form a baffle to fluid flow (Færseth 2006; Bastesen et al. 2010); fault-gouge and clay smear can significantly diminish the conductive properties of the fault, both across and along the fault plane.

## ***Fracture size***

The fracture size is defined by its vertical extent (height), lateral extent (length) and aperture (opening).

The length distribution of fractures is one of the principal controls on the connectivity and permeability of the fracture system (de Dreuzy et al. 2001; Philip et al. 2005). In the subsurface, the horizontal extent, or fracture length, cannot be readily measured below seismic scale, requiring the use of outcrop analogues for their elucidation. Alternatively, the size distribution of faults imaged using seismic reflection data can be extrapolated downscale using an assumed size distribution (Yielding 1996).

In the case-of non-stratabound fractures, there is no characteristic length scale that controls the size of the fractures, so their horizontal extent and maximum displacement tend to follow a power-law (Pareto) cumulative frequency distribution typical of fractals (Odling et al. 1999; Gillespie et al. 2001; Bertrand et al. 2015). In stratabound examples, the mechanical unit thickness typically imparts a characteristic spacing to the fractures (Bai and Pollard 2000; Schöpfer et al. 2011) and their length is controlled by interaction with other joints (Gross et al. 1993). This means that stratabound fractures tend not to follow non-power law size distributions and are not fractal (Gillespie et al. 1999). As stratabound fracture systems tend to divide the rock matrix into a series of blocks of regular size, the effective permeability of the fractured rock can be assigned a representative elementary

volume (Bear 1972; Odling et al. 1999; Müller et al. 2010). However, in fracture systems that have power law size distribution and clustered spatial distribution, the definition of representative elementary volume may not be possible.

The aperture of subsurface fractures is difficult to estimate directly and surface apertures may be unrepresentative of subsurface fractures due to the changing stress conditions occurring at different depths. However, partially cemented fractures have an aperture at the surface that is less sensitive to stress and so study of veins and partially cemented fractures can provide useful information (Laubach et al. 2016; Laubach 2019). In this context, it is important to distinguish between the distance between the fracture walls, or kinematic aperture and the true aperture which is the distance across the void within the fracture.

In a study of veins (fully cemented fractures) from a range of sedimentary rocks, Gillespie et al. (1999) concluded that veins typically have kinematic apertures that follow power law cumulative frequency distributions in non stratabound fracture systems, but they are non-power law in stratabound fracture systems. However, Ortega et al. (2006) reported stratabound fractures veins in carbonate host rocks and found them to have a power law kinematic aperture distribution. Additionally, Hooker et al. (2013, 2014) have demonstrated from detailed examination of fractures in sandstone that the process of fracture cementation can have a fundamental effect on the size distributions of fractures: power-law kinematic aperture size distributions are favoured in cases where fracture growth is unevenly distributed amongst variably cemented fractures.

In Type I fractured reservoirs, the fracture porosity dominates the storage potential of the reservoir and so accurate determination of the fracture size, including the fracture height, length and aperture, is critical for commercial development.

Comprehensive analyses of multi-scale size distributions of fractures are given from the Lewisian Complex by McCaffrey et al. (**this volume**), and from volcanics by Primaleon et al. (**this volume**). In both areas, composite cumulative frequency plots of fracture length show approximately power law distributions of several orders of magnitude, although in the poorly exposed volcanics (Primaleon et al. **this volume**), there is a marked change in exponent between regional scale datasets from maps and smaller scale data derived from outcrop and core. In each of these studies, the scaling of the fracture kinematic aperture (the distance between the fracture walls, regardless of fill) was also analysed. In both datasets, the kinematic aperture shows a broadly power-law cumulative frequency distribution, with higher observed frequencies of small aperture fractures in core data than in outcrop data. In the Lewisian rocks of the Lancaster discovery, subsurface aperture measurements derived from electrical logs also fall broadly onto a power-law cumulative frequency distribution when different samples are plotted onto a single graph, although individual samples do not conform to power-law size distributions. (Holdsworth et al. **this volume**).

### ***Joint density and lithology***

Opening-mode fractures (joints) cannot develop in cohesionless materials, and consideration of the Griffith/Navier-Coulomb failure criterion shows that rock with low cohesion, such as poorly cemented sand or porous carbonate grainstone, opening mode fractures can only develop under conditions of very low differential stress (e.g. Price and Cosgrove 1990). Hence opening mode fractures are rare or absent in high porosity reservoir sandstone or limestone unless they have been subjected to elevated pore-pressure. However, as cementation increases, porosity and pore throat sizes decrease and cohesion increases, making the rock become more brittle and prone to fracture. Thus, by pure serendipity, as the matrix loses permeability by cementation, the reservoir is more likely to have a component of fracture permeability. An example of this effect is seen in the Valhall chalk field, where fractured hardgrounds provide high permeability zones within the reservoir (Tjetland et al. 2007).

Surface and subsurface observations indicate that the density of joints varies strongly according to the brittleness of the rock at the time of deformation. As a rough guide, the relative brittleness of different rock types can be expressed as: silica > tight carbonate > porous carbonate > clay or organic-rich shale. Similarly, quartz-cemented sandstone is more prone to fracturing than porous sandstone. The presence of clay minerals can weaken the rock and make it significantly less brittle, so clay-rich carbonates tend to have lower fracture density than clean carbonates (Laubach et al. 2009).

### ***Fracture connectivity***

The connectivity of the fracture system is one of the most important controls on the effective permeability of fractured networks and has been investigated using percolation theory (Long and Witherspoon 1990). At low fracture density, fractures tend to be disconnected and so have limited contribution to effective permeability (but see also Philip et al. 2005 and Olson et al. 2009). At high density, the fractures are fully connected leading to a fracture system that is highly permeable. At intermediate density, fractures start to become connected and may form a number of isolated connected networks. The point at which the fracture system becomes connected across the reservoir is called the percolation threshold and is controlled by the total fracture density, the fracture size, and their orientation distribution (Hestir and Long 1990).

The number and type of fracture intersections are important factors in which influence fracture network connectivity. Measurements of fracture topology from core or from surface data allow rigorous quantification connectivity (Manzocchi 2002; Sanderson and Nixon 2015; Sanderson and Nixon 2018). Using these techniques, McCaffrey et al. (**this volume**) and Holdsworth et al. (**this volume**) showed high degree of connectivity of fractures in Lewisian basement at outcrop and at in the basement of the Rona Ridge. In a multiscale study of the volcanic rocks of the Southern Negros geothermal field, Primaleon et al. (**this volume**) found high fracture connectivity and were able to establish that connectivity is greater close to large faults. Unfortunately, the connectivity of the fracture

system to an individual well cannot be uniquely determined from static subsurface data alone, as the details of the fracture topology cannot be mapped far from the borehole. However, we can infer connectivity from pressure data, interference tests and the use of tracers (see Narr et al. 2006 and Price et al. **this volume** for examples).

### ***Factors causing fracture localization***

An important aspect of fractured reservoir characterisation is the understanding of the factors that cause localization and change in orientation of fractures. Regions that are highly fractured often represent high-permeability zones, which could act as areas of high well productivity, or areas of early breakthrough of injected water or gas. In the former case it pays to target highly fractured regions, whereas in the latter they should be avoided; getting this right or wrong can determine the commercial success or failure of a field.

The damage zone model of fault-related fracturing is widely used in reservoir modelling (e.g. Gauthier et al. 2002) and implies localized high permeability zones of open fractures associated with faults. However, stratabound joints that form when the faults are active may be more homogeneously distributed, with their orientation determined by local stress perturbations around the faults (e.g. Rawnsley et al. 1992; Bourne et al. 2001).

Clusters of opening mode fractures, or fracture corridors, may be due to local stress concentrations, such as may occur close to faults. However, in many cases there are no obvious causes of stress heterogeneity. Olson (2004) has shown using mechanical modelling that clusters of joints may occur spontaneously in a growing set of fractures due to the interaction of the stress fields around each fracture. Hence prediction of fracture corridors is challenging and there is a reliance instead on direct detection using well data or seismic techniques (Ozkaya 2007; Nosjean et al. 2020).

Folding can cause localization of fracturing. For example, in the thrust-related folds of the Canadian foothills, successful gas wells are targeted into the hinges or forelimbs of folds (Cooper et al. 2004). However, not all the fractures in a fold are related to the folding event; some may have developed before and others after the event, in which case their fracture density and orientation may not be related to fold geometry (Ahmadhadi et al. 2008; Shackleton et al. 2011; Casini et al. 2011; Tavani et al. 2018).

Various techniques can be used to predict fracture density and orientation. In a simple static approach, the curvature of horizons may be used to estimate fracture density (Stewart & Podolski 1998; Bergbauer & Pollard 2003). In faulted areas, the distance from faults may be used to condition the density of fractures. Otherwise, geomechanical modelling can be used to estimate the stress/strain at the time of deformation, and thereby to estimate fracture parameters (Bourne et al. 2001; Maerten et al. 2019). Regardless of the technique that is used, results must be carefully calibrated against seismic and well data and supported by outcrop analogue data where appropriate.

### ***In situ stress***

The orientation and magnitudes of *in-situ* stress can have a significant impact on fracture aperture, and hence the effective permeability tensor of fractured formations. As the reservoir fluid pressure is depleted, the effective stress changes and fractures may close, becoming less permeable: such reservoirs are called “stress-sensitive”. However, rough walled or partially filled cemented fractures may become locked open, or propped, making the reservoirs less sensitive to stress (Dyke and Hudson 1992).

Wellbore temperature monitoring in fractured crystalline basement has shown that the fractures most likely to be open and permeable are those that are oriented relative to stress field in such a way that they are on the verge of slipping, leading to the concept of “critically stressed” fractures (Barton et al. 1995). Gilchrist et al. (**this volume**) give evidence that in the carbonates of the Shaikan field in Kurdistan, the fractures remain critically stressed even after depletion of the reservoir; they argue that, in such seismically active regions, the tectonic stress will build up again until the system reaches criticality. The continued criticality of the fracture system may allow the reservoir to maintain high effective permeability during depletion, but the critically stressed fractures may also present problems for wellbore integrity.

### ***Chemical modification of fractured systems***

Carbonate reservoirs often have a complex diagenetic history, with diagenetic processes frequently controlled or influenced by phases of fracturing (Smith and Davies 2006; Sharp et al. 2010). When carbonate rocks are exposed in a humid environment, or under certain conditions in the subsurface, they may undergo dissolution to form karst (Loucks 1999, White 2016), a phenomenon in which carbonate or evaporite minerals are dissolved to form macroscopic vugs and caves. Karst dissolution enlarges the aperture of pre-existing fractures with an increase in porosity and permeability. However, porosity may also become blocked by sediment or by precipitation of diagenetic minerals. As a result, karst reservoirs are often complex. They share many of the production characteristics of fractured reservoirs, although the additional presence of open voids and caverns can lead to extremely heterogeneous production characteristics and reservoir behaviour. Drill-bit drops and high instantaneous mud-loss rates are typical experiences in highly karstified reservoirs (Mazullo and Chilingarian 1996; Loucks 1999).

Under some conditions, dissolution of carbonates can occur in the deep subsurface (Mazzulo and Harris 1992), although there is controversy around whether this process can generate significant porosity (Ehrenberg et al. 2012). Nevertheless, there is evidence that late-stage dissolution and vug formation can occur at depth in association with fractures. Ukar et al. (**this volume**) argue that in the Halahatang oilfield of the Tarim Basin, which is hosted by Ordovician carbonate rocks, cavernous porosity developed at moderate depths in a series of dissolution events.

Caverns developed by karst dissolution of carbonate or evaporite can collapse, causing intense fracturing and brecciation of the overlying rocks (e.g. Daniels et al. 2020, Ukar et al. **this volume**). These zones can be associated with enhanced production rates, as found in the Ellenburger Group carbonates of Texas (Loucks 1999).

Early and pervasive cementation of the carbonate platform causes embrittlement, leading to the development of major syn-depositional fracture systems behind the margin of steep-sided platforms (Hunt et al. 2003, Frost and Kerans 2010, Nolting et al. 2020). This can have important consequences for production, for example in the Paleozoic super-giant Tengiz field in Kazakhstan (Narr and Flodin 2012), and the Devonian-aged Kharyaga field in Russia, (Spina et al. 2015).

Crystalline basement is, by its nature, rock of very low porosity and permeability, which depending on mineralogy commonly has low chemical reactivity. Development of fractures in crystalline basement may not provide sufficient storage for commercial reservoir potential, as the porosity of unaltered fractures is very low. Some degree of chemical alteration may therefore be required to generate a hydrocarbon reservoir, and this may be provided by chemical weathering if the basement is exposed over a very long time. Therefore, productive basement reservoirs typically underlie major unconformities (P'An 1982; Koning 2003; Holdsworth et al. **this volume**). Fractures formed close to the weathering surface may form open fissures that extend down into the underlying basement and focus descending or ascending fluids, leading to fracture porosity and permeability enhancement by chemical and mechanical weathering.

Hydrothermal alteration is commonly observed in crystalline basement rocks. In some geothermal reservoirs, hydrothermal circulation allows the precipitation of geothermal minerals that can prop open or occlude the fractures. In Soultz-sous-Forêts the wall rocks of the fractures have been intensely transformed by hydrothermal alteration and the mineral assemblage must be characterized in order to design the best stimulation (Ledéseret et al. 2010). In the Lancaster oil field of the UK's Rona ridge, a near surface hydrothermal system was associated with fractures in the basement (Holdsworth et al. **this volume**). The hydrothermal minerals that were generated from this system propped open the fissures, allowing storage of oil.

## **Data acquisition**

The subsurface data available for the characterisation of fracture networks consists of seismic data and well data. Seismic reflection data are of limited spatial resolution, and as such can only image large faults. Well data are of much higher resolution, but do not capture the key characteristics of any of the larger fractures. Between seismic data and well data exists a range of scales at which fractures cannot be directly sampled. This is known as the resolution gap, for which outcrop analogues and remote sensing can provide important proxy data.

Seismic reflection data are important for mapping the larger structures such as faults, although the vast majority of fractures will not be directly detectable. Seismic anisotropy can also be used to infer the presence and orientation of fractures under suitable conditions. Newly developed methods for extracting faults and fractures from seismic data are showing promise and can be a useful adjunct to manual interpretation (e.g. Bonter and Trice 2019; Wu et al. 2019).

Core provides essential information about the content of fractures and the density and small-scale connectivity of the fracture network. CT scans of core can yield 3-D volume renditions of the fractures in the core barrel, before the core is damaged by further handling (Wennberg et al. 2009). However, the most intensely fractured reservoir intervals typically result in zones of no recovery or ‘rubble zones’ and so are under-sampled by coring.

Borehole imagery allows the determination of fracture orientation and properties (Poppelreiter et al. 2010), and the quality of borehole images is steadily improving. Acoustic and resistivity-based tools are both valuable and yield complementary results and integration with core data can provide calibration of the results (Fernández-Ibáñez et al. 2018). Borehole imagery is also used to determine the direction of *in situ* stress, which can affect fracture permeability (e.g. Gilchrist et al. **this volume**).

In the absence of borehole imagery, conventional wireline logs can provide information about fracturing. For instance, the caliper, sonic and photoelectric logs are all sensitive to fracturing and can indicate fractured zones in the well.

While information about the size and connectivity of fractures is very limited from well data, outcrops can provide a wealth of data about the extent of fractures, their fills and their relation to lithology and geological structure. Fieldwork can be supplemented by the use of remote sensing data, and also increasingly by virtual outcrop models derived from LiDAR or from drone-based digital photogrammetry (e.g. Pearce et al. 2011; Gillespie et al. 2011; Vollgger and Cruden 2016; Corradetti et al. 2018).

Dynamic data such as production tests and interference tests are essential for determination of the effective permeability. Mud losses and gas kicks can also provide dynamic information about the fracture system (Alvarez et al. 2015), with use of systems such as real time mud gas monitoring micro mud-loss meters that are designed to optimize collection of this information.

In an optimal workflow, the fracture network is represented as a discrete fracture network (DFN) and the pressure derivative of the well test is matched by adjusting the matrix and fracture parameters. In this way, the geological and engineering concept of the fractured reservoir can be fully integrated. A good example of this workflow applied to the fractured carbonate Shaikan field is given in Price et al. (**this volume**). DFNs were created for individual well tests using all of the available geological data and adjusted to match the well test pressure derivatives. The DFNs were then validated by simulation of transient bottom hole pressures and pressure interference data. The field scale DFN was then upscaled to a full-field dynamic simulation model for use in production forecasting.

## **Conclusions**

An understanding of the geological controls on fracture system development and organisation is fundamental to developing viable concepts of fracturing that can be used in assessing fractured hydrocarbon and geothermal reservoirs. Host rock lithology and stress conditions effect the organization and scaling of fracture systems and the development of



653 stratabound, non-stratabound or hierarchical fracture systems. The degree of chemical  
654 modification depends on the primary composition of the host rock as well as on the  
655 geofluids that were present. When fractures occur at the surface they may be strongly  
656 altered and may be filled with sediment, altering their hydraulic properties. Use of data  
657 from core and outcrop analogues is important for understanding the geological  
658 development of fractures, but the addition of other data sources such as seismic, borehole  
659 image data and dynamic data allows for a more complete definition of the hydraulic effect  
660 of the fracture systems.

661 The papers in this volume intend to give some good examples of how a proper geological  
662 understanding and quantitative analysis of fracture systems improves our ability to make  
663 useful predictions in the subsurface.

#### 664 **Acknowledgements**

666 Ole Petter Wennberg and Long Wu thanked for their constructive comments on the  
667 manuscript. Stephen Laubach is thanked for his detailed review.

## References

- Agosta, F. (2008). Fluid flow properties of basin-bounding normal faults in platform carbonates, Fucino Basin, central Italy. *Geological Society, London, Special Publications*, 299(1), 277-291.
- Ahmadhadi, F., Lacombe, O., & Daniel, J. M. (2007). Early reactivation of basement faults in Central Zagros (SW Iran): evidence from pre-folding fracture populations in Asmari Formation and lower Tertiary paleogeography. In *Thrust Belts and Foreland Basins* (pp. 205-228). Springer, Berlin, Heidelberg.
- Allan, J., & Sun, S. Q. (2003). Controls on recovery factor in fractured reservoirs: lessons learned from 100 fractured fields. In *SPE Annual Technical Conference and Exhibition*. Society of Petroleum Engineers.
- Alvarez, S. F., Cazuriaga, G. V., Martocchia, A., & Chamon, O. (2015). Evaluation of a Fractured Tight Reservoir in Real-Time: The Importance of Detecting Open Fractures while Drilling with Accurate Mud Flow Measurement. *AAPG# 2102787. Denver, CO, USA*.
- Anders, M. H., Laubach, S. E., & Scholz, C. H. (2014). Microfractures: A review. *Journal of Structural Geology*, 69, 377-394.
- Anderson E.M. (1904) The dynamics of faulting. *Transactions of the Edinburgh Geological Society*, 8, 387-402, <https://doi.org/10.1144/transed.8.3.387>
- Bai, T., & Pollard, D. D. (2000). Fracture spacing in layered rocks: a new explanation based on the stress transition. *Journal of Structural Geology*, 22(1), 43-57.
- Barbier, E. (1997). Nature and technology of geothermal energy: a review. *Renewable and sustainable energy reviews*, 1(1-2), 1-69.
- Barton, C. A., Zoback, M. D., & Moos, D. (1995). Fluid flow along potentially active faults in crystalline rock. *Geology*, 23(8), 683-686.

Bastesen, E., & Braathen, A. (2010). Extensional faults in fine grained carbonates—analysis of fault core lithology and thickness—displacement relationships. *Journal of Structural Geology*, 32(11), 1609-1628.

Bear J (1972) Dynamics of fluids in porous media. Environmental science series. Elsevier, Amsterdam, p 784.

Bense, V. F., Gleeson, T., Loveless, S. E., Bour, O., & Scibek, J. (2013). Fault zone hydrogeology. *Earth-Science Reviews*, 127, 171-192.

Bergbauer, S. & Pollard, D.D. 2003. How to calculate normal curvatures of sampled geological surfaces. *Journal of Structural Geology*, 25, 277–289.

Bertotti, G., Hardebol, N., Taal-van Koppen, J. K., & Luthi, S. M. (2007). Toward a quantitative definition of mechanical units: New techniques and results from an outcropping deep-water turbidite succession (Tanqua-Karoo Basin, South Africa). *AAPG bulletin*, 91(8), 1085-1098.

Bertrand, L., Géraud, Y., Le Garzic, E., Place, J., Diraison, M., Walter, B. & Haffen, S. (2015). "A multiscale analysis of a fracture pattern in granite: A case study of the Tamariu granite, Catalunya, Spain." *Journal of Structural Geology* 78, 52-66.

Biddle, K. T. and Wielchowsky, C. C., 1994. Hydrocarbon Traps: Chapter 13: Part III. Processes. In: Magoon, L. & Dow, W. (ed.) The Petroleum System - From Source To Trap. AAPG Memoir 60, 219-235.

Bonter, D. A., & Trice, R. (2019). An integrated approach for fractured basement characterization: the Lancaster Field, a case study in the UK. *Petroleum Geoscience*, 25(4), 400-414.

Bourne, S.J., Rijkels, L, Stephenson, B.J., Willemse, E.J.M. 2001. Predictive modelling of naturally fractured reservoirs using geomechanics and flow simulation. *GeoArabia*, 6, p 27-42.

C&C Reservoirs (2020), DAKS 4.0. Unpublished.

739 Caine, J. S., Evans, J. P., & Forster, C. B. (1996). Fault zone architecture and permeability  
740 structure. *Geology*, 24(11), 1025-1028.

741 Casini, G., Gillespie, P. A., Vergés, J., Romaine, I., Fernández, N., Casciello, E., ... & Aghajari, L.  
742 (2011). Sub-seismic fractures in foreland fold and thrust belts: insight from the Lurestan  
743 Province, Zagros Mountains, Iran. *Petroleum Geoscience*, 17(3), 263-282.

744

745 Cooper, M., C. Brealey, P. Fermor, R. Green, and M. Morrison, 2004, Structural models of  
746 subsurface thrust-related folds in the foothills of British Columbia— Case studies of  
747 sidetracked gas wells, in K. R. McClay, ed., *Thrust tectonics and hydrocarbon systems: AAPG*  
748 *Memoir* 82, p. 579–597.

749

750 Corbett, K., Friedman, M., & Spang, J. (1987). Fracture development and mechanical  
751 stratigraphy of Austin Chalk, Texas. *AAPG Bulletin*, 71(1), 17-28.

752

753 Corradetti, A., S. Tavani, M. Parente, A. Iannace, F. Vinci, C. Pirmez, S. Torrieri, M. Giorgioni,  
754 A. Pignalosa, and S. Mazzoli. (2018) "Distribution and arrest of vertical through-going joints  
755 in a seismic-scale carbonate platform exposure (Sorrento peninsula, Italy): insights from  
756 integrating field survey and digital outcrop model." *Journal of Structural Geology* 108, 121-  
757 136.

758

759 Cotton, L., Gutmanis, J., Shail, R., Dalby, C., Batchelor, T., Foxford, A. and G. Rollinson. (2020)  
760 Geological overview of the United Downs deep geothermal power project, Cornwall, UK.  
761 Proceedings World Geothermal Congress, Reykjavik, Iceland, April 26 – May 2, 2020.

762

763 Crawford, B. R., & Yale, D. P. (2002). Constitutive modeling of deformation and permeability:  
764 relationships between critical state and micromechanics. In *SPE/ISRM Rock Mechanics*  
765 *Conference*. Society of Petroleum Engineers.

766

767 Cuong, T. X., & Warren, J. K. (2009). Bach ho field, a fractured granitic basement reservoir,  
768 Cuu Long Basin, offshore SE Vietnam: A “buried-hill” play. *Journal of Petroleum*  
769 *Geology*, 32(2), 129-156.

770

771 Dalrymple, G. B., Grove, M., Lovera, O. M., Harrison, T. M., Hulen, J. B., & Lanphere, M. A.  
772 (1999). Age and thermal history of the Geysers plutonic complex (felsite unit), Geysers  
773 geothermal field, California: a <sup>40</sup>Ar/<sup>39</sup>Ar and U–Pb study. *Earth and Planetary Science*  
774 *Letters*, 173(3), 285-298.

775

776 Daniel, E. J. 1954. Fractured Reservoirs of Middle East. Bulletin of the American Association  
777 of Petroleum Geologists, 38(5), 774–815.

778

779 Daniels, S.E., Tucker, M.E., Mawson, M.J., Holdsworth, R.E., Long, J.J., Gluyas, J.G. and Jones,  
780 R.R. 2020. Nature and origin of collapse breccias in the Zechstein of NE England: local  
781 observations with cross-border petroleum exploration and production significance, across  
782 the North Sea. In: Georgiopoulou, A., et al. (eds) *Subaqueous Mass Movements and their*  
783 *Consequences: Advances in Process Understanding, Monitoring and Hazard Assessments*.  
784 Geological Society, London, Special Publications, 494, [https://doi.org/10.1144/SP494-2019-](https://doi.org/10.1144/SP494-2019-140)  
785 [140](https://doi.org/10.1144/SP494-2019-140)

786

787 de Dreuzy, J. R., Davy, P., & Bour, O. (2001). Hydraulic properties of two-dimensional  
788 random fracture networks following a power law length distribution: 2. Permeability of  
789 networks based on lognormal distribution of apertures. *Water Resources Research*, 37(8),  
790 2079-2095.

791

792 De Keijzer, M., Hillgartner, H., Al Dhahab, S., & Rawnsley, K. (2007). A surface-subsurface  
793 study of reservoir-scale fracture heterogeneities in Cretaceous carbonates, North  
794 Oman. Geological Society, London, Special Publications, 270(1), 227-244.

795

796 Dyke, C. G. and Hudson, J.A. (1992). Stress insensitive natural fracture permeability within  
797 hydrocarbon reservoirs. In *Rock Characterization: ISRM Symposium, Eurock'92, Chester, UK,*  
798 *14–17 September 1992* (pp. 281-286). Thomas Telford Publishing.

799

800 Ehrenberg, S. N., Walderhaug, O., & Bjørlykke, K. (2012). Carbonate porosity creation by  
801 mesogenetic dissolution: Reality or illusion? *AAPG bulletin*, 96(2), 217-233.

802

803 Engelder, T. 1993. Stress Regimes in the Lithosphere. Princeton University Press, pp. 457.

804

805 Færseth, R. B. (2006). Shale smear along large faults: continuity of smear and the fault seal  
806 capacity. *Journal of the Geological Society*, 163(5), 741-751.

807

808

809 Feng, Z. Q. (2008). Volcanic rocks as prolific gas reservoir: A case study from the Qingshen  
810 gas field in the Songliao Basin, NE China. *Marine and Petroleum Geology*, 25(4-5), 416-432.

811

Fernández-Ibáñez, F., DeGraff, J. M., & Ibrayev, F. (2018). Integrating borehole image logs with core: A method to enhance subsurface fracture characterization. *AAPG Bulletin*, 102(6), 1067-1090.

Ferrill, D.A., McGinnis, R.N., Morris, A.P., Smart, K.J., Sickmann, Z.T., Bents, M., Lehrmann, D and Evans, M.A. 2014. Control of mechanical stratigraphy on bed-restricted jointing and normal faulting: Eagle Ford Formation, south-central Texas. *AAPG Bulletin* 98, 2477–2506.

Fossen, H., Schultz, R. A., & Torabi, A. (2011). Conditions and implications for compaction band formation in the Navajo Sandstone, Utah. *Journal of Structural Geology*, 33(10), 1477-1490.

Foster, M. E., & Hudleston, P. J. (1986). “Fracture cleavage” in the Duluth Complex, northeastern Minnesota. *Geological Society of America Bulletin*, 97(1), 85-96.

Frost III, E. L., & Kerans, C. (2010). Controls on syndepositional fracture patterns, Devonian reef complexes, Canning Basin, Western Australia. *Journal of Structural Geology*, 32(9), 1231-1249.

Gale, J. F., Lander, R. H., Reed, R. M., & Laubach, S. E. (2010). Modeling fracture porosity evolution in dolostone. *Journal of Structural Geology*, 32(9), 1201-1211.

Gale, J. F., Laubach, S. E., Olson, J. E., Eichhubl, P., & Fall, A. (2014). Natural fractures in shale: A review and new observations. *Natural Fractures in Shale: A Review and New Observations*. AAPG bulletin, 98(11), 2165-2216.

Gauthier, B. D. M., Auzias, V., Garcia, M., & Chiapello, E. (2002, January). Static and dynamic characterization of fracture pattern in the Upper Jurassic reservoirs of an offshore Abu Dhabi field: From well data to full field modeling. In *Abu Dhabi International Petroleum Exhibition and Conference*. Society of Petroleum Engineers.

Gillespie, P.A., Howard, C., Walsh, J.J. & Watterson, J., 1993. Measurement and characterisation of spatial distributions of fractures. *Tectonophysics*. 226 113-141.

Gillespie, P.A., Johnston, J.D., Loriga, M.A., McCaffrey, K.L.W., Walsh, L.L., Watterson, L., 1999. Influence of layering on vein systematics in line samples. In: McCaffrey, K.J.W., Lonergan, L., Wilkinson, J.J. (Eds.), *Fractures, Fluid Flow and Mineralization*. Geological Society, London, Special Publication 155, pp. 35-56.

Gillespie, P.A., Walsh, J.J., Watterson, J., Bonson, C.G. & Manzocchi, T. 2001. Scaling relationships of joints and vein arrays from The Burren, Co. Clare, Ireland. *Journal of Structural Geology*, 23, 183-202.

- Gillespie, P. A., Monsen, E., Maerten, L., Hunt, D., Thurmond, J., Tuck, D. & Sullivan, M. D. (2011). Fractures in carbonates: From digital outcrops to mechanical models. *Outcrops revitalized—Tools, techniques and applications: Tulsa, Oklahoma, SEPM Concepts in Sedimentology and Paleontology*, 10, 137-147.
- Graham Wall, B. R., Girbacea, R., Mesonjesi, A., & Aydin, A. (2006). Evolution of fracture and fault-controlled fluid pathways in carbonates of the Albanides fold-thrust belt. *AAPG Bulletin*, 90(8), 1227-1249.
- Gross, M. R. (1993). The origin and spacing of cross joints: examples from the Monterey Formation, Santa Barbara Coastline, California. *Journal of Structural Geology*, 15(6), 737-751.
- Gross, M. R., Fischer, M. P., Engelder, T., & Greenfield, R. J. (1995). Factors controlling joint spacing in interbedded sedimentary rocks: integrating numerical models with field observations from the Monterey Formation, USA. Geological Society, London, Special Publications, 92(1), 215-233.
- Gross, M. R., 1998, Practical methods of fracture analysis - implications for fractured reservoirs: in, Hoak, T.E., ed., *Fractured Reservoirs: Practical Exploration and Development Strategies*, Rocky Mountain Assoc. of Geologists, p. 117-136.
- Gudmundsson, A., & Løtveit, I. F. (2014). Sills as fractured hydrocarbon reservoirs: examples and models. *Geological Society, London, Special Publications*, 374(1), 251-271.
- Gutmanis, J., i Oró, L. A., Díez-Canseco, D., Chebbihi, L., Awdal, A., & Cook, A. (2018). Fracture analysis of outcrop analogues to support modelling of the subseismic domain in carbonate reservoirs, south-central Pyrenees. Geological Society, London, Special Publications, 459(1), 139-156.
- Healy, D. and Blenkinsop, T. and Timms, N.E. and Meredith, P. and Mitchell, T. and Cooke, M. (2015). Polymodal faulting: Time for a new angle on shear failure. *Journal of Structural Geology*. 80: pp. 57-71.
- Hestir, K., & Long, J. C. (1990). Analytical expressions for the permeability of random two-dimensional Poisson fracture networks based on regular lattice percolation and equivalent media theories. *Journal of Geophysical Research: Solid Earth*, 95 (B13), 21565-21581.
- Hetényi, G., Taisne, B., Garel, F., Médard, É., Bosshard, S., & Mattsson, H. B. (2012). Scales of columnar jointing in igneous rocks: field measurements and controlling factors. *Bulletin of Volcanology*, 74(2), 457-482.
- Holdsworth, R.E., McCaffrey, K.J.W., Dempsey, E., Roberts, N.M.W., Hardman, K., Morton, A., Feely, M., Hunt, J., Conway, A., Robertson, A. 2019. Natural fracture propping and

897 earthquake-induced oil migration in fractured basement reservoirs. *Geology*, 47,  
898 <https://doi.org/10.1130/G46280.1>

899

900 Hooker, J. N., Laubach, S. E., & Marrett, R. (2013). Fracture-aperture size—Frequency,  
901 spatial distribution, and growth processes in strata-bounded and non-strata-bounded  
902 fractures, Cambrian Mesón Group, NW Argentina. *Journal of Structural Geology*, 54, 54-71.

903

904 Hooker, J.N., Laubach, S.E., and Marrett, R., 2014. A universal power-law scaling exponent  
905 for fracture apertures in sandstone. *Geological Society of America Bulletin* 126(9-10), 1340-  
906 1362. doi: 10.1130/B30945.1

907

908 Huang, Q., Angelier, L., 1989. Fracture spacing and its relation to bed thickness. *Geological*  
909 *Magazine* 126, 550-556.

910

911 Hunt, D. W., Fitchen, W. M., & Kosa, E. (2003). Syndepositional deformation of the Permian  
912 Capitan reef carbonate platform, Guadalupe Mountains, New Mexico, USA. *Sedimentary*  
913 *Geology*, 154(3-4), 89-126.

914

915 Johri, M., Zoback, M. D., & Hennings, P. (2014). A scaling law to characterize fault-damage  
916 zones at reservoir depths. *AAPG Bulletin*, 98(10), 2057-2079.

917

918 Kaminskaite, I., Fisher, Q. J., & Michie, E. A. H. (2019). Microstructure and petrophysical  
919 properties of deformation bands in high porosity carbonates. *Journal of Structural*  
920 *Geology*, 119, 61-80.

921

922 Kim, Y. S., Peacock, D. C. P., & Sanderson, D. J. (2003). Mesoscale strike-slip faults and  
923 damage zones at Marsalforn, Gozo Island, Malta. *Journal of Structural Geology*, 25(5), 793-  
924 812.

925

926 Koning, T. (2003). Oil and gas production from basement reservoirs: examples from  
927 Indonesia, USA and Venezuela. *Geological Society, London, Special Publications*, 214(1), 83-  
928 92.

929

930 Laubach, S. E. (2003). Practical approaches to identifying sealed and open fractures. *AAPG*  
931 *bulletin*, 87(4), 561-579.



932

933 Laubach, S. E., Reed, R. M., Olson, J. E., Lander, R. H., & Bonnell, L. M. (2004). Coevolution of  
934 crack-seal texture and fracture porosity in sedimentary rocks: cathodoluminescence  
935 observations of regional fractures. *Journal of Structural Geology*, 26(5), 967-982.

936

937 Laubach, S. E., Olson, J. E., & Gross, M. R. (2009). Mechanical and fracture stratigraphy.  
938 *AAPG bulletin*, 93 (11), 1413-1426.

939

940 Laubach, S. E., Fall, A., Copley, L. K., Marrett, R., & Wilkins, S. J. (2016). Fracture porosity creation  
941 and persistence in a basement-involved Laramide fold, Upper Cretaceous Frontier Formation, Green  
942 River Basin, USA. *Geological Magazine*, 153(5-6), 887-910.

943

944 Laubach, S. E., Lamarche, J., Gauthier, B. D., Dunne, W. M., & Sanderson, D. J. (2018). Spatial  
945 arrangement of faults and opening-mode fractures. *Journal of Structural Geology*, 108, 2-15.

946

947 Laubach, S.E., Lander, R.H., Criscenti, L.J., et al., 2019. The role of chemistry in fracture  
948 pattern development and opportunities to advance interpretations of geological materials.  
949 *Reviews of Geophysics*, 57 (3), 1065-1111. doi:10.1029/2019RG000671

950

951 Ledésert, B., Hebert, R., Genter, A., Bartier, D., Clauer, N., & Grall, C. (2010). Fractures,  
952 hydrothermal alterations and permeability in the Soultz Enhanced Geothermal  
953 System. *Comptes Rendus Geoscience*, 342(7-8), 607-615.

954

955 Li, J. Z., Laubach, S. E., Gale, J. F. W., & Marrett, R. A. (2018). Quantifying opening-mode  
956 fracture spatial organization in horizontal wellbore image logs, core and outcrop: application  
957 to Upper Cretaceous Frontier Formation tight gas sandstones, USA. *Journal of Structural*  
958 *Geology*, 108, 137-156.

959

960 Lima, B. E. M., & De Ros, L. F. (2019). Deposition, diagenetic and hydrothermal processes in  
961 the Aptian Pre-Salt lacustrine carbonate reservoirs of the northern Campos Basin, offshore  
962 Brazil. *Sedimentary Geology*, 383, 55-81.

963

964 Long, J. C., & Witherspoon, P. A. (1985). The relationship of the degree of interconnection to  
965 permeability in fracture networks. *Journal of Geophysical Research: Solid Earth*, 90(B4),  
966 3087-3098.

967

968 Loucks, R. G. (1999). Paleocave carbonate reservoirs: Origins, burial-depth modifications,  
969 spatial complexity, and reservoir implications. *AAPG bulletin*, 83(11), 1795-1834.

970

971 Lu, S. M. (2018). A global review of enhanced geothermal system (EGS). *Renewable and*  
972 *Sustainable Energy Reviews*, 81, 2902-2921.

973

974 Maerten, L., Legrand, X., Castagnac, C., Lefranc, M., Joonnekindt, J. P., & Maerten, F. (2019).  
975 Fault-related fracture modeling in the complex tectonic environment of the Malay basin,  
976 offshore Malaysia: an integrated 4D geomechanical approach. *Marine and Petroleum*  
977 *Geology*, 105, 222-237.

978

979 Magara, K. (2003). Volcanic reservoir rocks of northwestern Honshu Island,  
980 Japan. *Geological Society, London, Special Publications*, 214(1), 69-81.

981

982 Manzocchi, T. (2002). The connectivity of two-dimensional networks of spatially correlated  
983 fractures. *Water Resources Research*, 38(9), 1-1.

984

985 Mazzullo, S. J., & Harris, P. M. (1992). Mesogenetic dissolution: its role in porosity  
986 development in carbonate reservoirs. *AAPG bulletin*, 76(5), 607-620.

987

988 Mazzullo, S. J., & Chilingarian, G. V. (1996). Hydrocarbon reservoirs in karsted carbonate  
989 rocks. In *Developments in Petroleum Science* (Vol. 44, pp. 797-865). Elsevier.

990

991 McNamara, D. D., Massiot, C., & Milicich, S. M. (2017). Characterizing the subsurface  
992 structure and stress of New Zealand's geothermal fields using borehole images. *Energy*  
993 *Procedia*, 125, 273-282.

994

995 Micarelli, L., Benedicto, A., & Wibberley, C. A. J. (2006). Structural evolution and  
996 permeability of normal fault zones in highly porous carbonate rocks. *Journal of Structural*  
997 *Geology*, 28(7), 1214-1227.

998

999 Morris, A. P., Ferrill, D. A., & McGinnis, R. N. (2009). Mechanical stratigraphy and faulting in  
1000 Cretaceous carbonates. *AAPG bulletin*, 93(11), 1459-1470.

1001

1002 Müller, C., Siegesmund, S., & Blum, P. (2010). Evaluation of the representative elementary  
1003 volume (REV) of a fractured geothermal sandstone reservoir. *Environmental earth*  
1004 *sciences*, 61(8), 1713-1724.

1005

1006 Narr, W., & Suppe, J. (1991). Joint spacing in sedimentary rocks. *Journal of Structural*  
1007 *Geology*, 13(9), 1037-1048.

1008

1009 Narr, W., & Flodin, E. (2012, April). Fractures in steep-rimmed carbonate platforms:  
1010 Comparison of Tengiz Reservoir, Kazakhstan, and outcrops in Canning Basin, NW Australia.  
1011 In *American Association of Petroleum Geologists, Annual Convention and Exhibition, Long*  
1012 *Beach, California*.

1013

1014 Narr, W., Schechter, D. S., & Thompson, L. B. (2006). *Naturally fractured reservoir*  
1015 *characterization* (Vol. 112). Richardson, TX: Society of Petroleum Engineers.

1016

1017 Nelson, R. (2001). *Geologic analysis of naturally fractured reservoirs*. Elsevier.

1018

1019 Nguyen, N. T. B., Dang, C. T. Q., Bae, W., Chen, Z., Nguyen, A., & Thuoc, P. H. (2011,  
1020 January). Geological characteristics and integrated development plan for giant naturally  
1021 fractured basement reservoirs. In *Canadian Unconventional Resources Conference*. Society  
1022 of Petroleum Engineers 149510.

1023

1024 Nixon, C. W., Vaagan, S., Sanderson, D. J., & Gawthorpe, R. L. (2019). Spatial distribution of  
1025 damage and strain within a normal fault relay at Kilve, UK. *Journal of Structural*  
1026 *Geology*, 118, 194-209.

1027

1028 Nolting, A., Zahm, C. K., Kerans, C., & Alzayer, Y. (2020). The influence of variable  
1029 progradation to aggradation ratio and facies partitioning on the development of  
1030 syndepositional deformation in steep-walled carbonate platforms. *Marine and Petroleum*  
1031 *Geology*, 114, 104171.

1032

1033 Nosjean, N., Khamitov, Y., Rodriguez, S., & Yahia-Cherif, R. (2020). Fracture corridor  
1034 identification through 3D multifocusing to improve well deliverability, an Algerian tight  
1035 reservoir case study. *Solid Earth Sciences*, 5(1), 31-49.

1036

1037 Odling, N. E., Gillespie, P., Bourguine, B., Castaing, C., Chiles, J. P., Christensen, N. P., ... &  
1038 Trice, R. (1999). Variations in fracture system geometry and their implications for fluid flow  
1039 in fractures hydrocarbon reservoirs. *Petroleum Geoscience*, 5(4), 373-384.

1040

1041 Olson, J. E. (2004). Predicting fracture swarms—The influence of subcritical crack growth  
1042 and the crack-tip process zone on joint spacing in rock. Geological Society, London, Special  
1043 Publications, 231(1), 73-88.

1044

1045 Olson, J. E., Laubach, S. E., & Lander, R. H. (2009). Natural fracture characterization in tight gas  
1046 sandstones: Integrating mechanics and diagenesis. *AAPG bulletin*, 93(11), 1535-1549.

1047

1048 Ortega, O. J., Marrett, R. A., & Laubach, S. E. (2006). A scale-independent approach to fracture  
1049 intensity and average spacing measurement. *AAPG bulletin*, 90(2), 193-208.

1050

1051 Ozkaya, S. I. (2007). Detection of fracture corridors from openhole logs in horizontal wells.  
1052 In SPE Saudi Arabia Section Technical Symposium. Society of Petroleum Engineers.

1053

1054 P'an, C. H. (1982). Petroleum in basement rocks. *AAPG Bulletin*, 66(10), 1597-1643.

1055

1056 Paul, P. K., Zoback, M. D., & Hennings, P. H. (2009). Fluid flow in a fractured reservoir using a  
1057 geomechanically constrained fault-zone-damage model for reservoir simulation. *SPE*  
1058 *Reservoir Evaluation & Engineering*, 12(04), 562-575.

1059

1060 Philip, Z. G., Jennings Jr, J. W., Olson, J. E., & Holder, J. (2005). Modeling coupled fracture-  
1061 matrix fluid flow in geomechanically simulated fracture networks. In SPE Annual Technical  
1062 Conference and Exhibition. Society of Petroleum Engineers.

1063

1064 Pearce, M. A., Jones, R. R., Smith, S. A., & McCaffrey, K. J. (2011). Quantification of fold  
1065 curvature and fracturing using terrestrial laser scanning. *AAPG Bulletin*, 95(5), 771-794.

1066

1067 Poppelreiter, M., Garcia-Carballido, C., & Kraaijveld, M. (2010). Borehole image log  
1068 technology: application across the exploration and production life cycle.

1069

Price, N. J., & Cosgrove, J. W. (1990). Analysis of geological structures. Cambridge University Press.

Pyrak-Nolte, L. J., & Morris, J. P. (2000). Single fractures under normal stress: The relation between fracture specific stiffness and fluid flow. *International Journal of Rock Mechanics and Mining Sciences*, 37(1-2), 245-262.

Questiaux, J. M., Couples, G. D., & Ruby, N. (2010). Fractured reservoirs with fracture corridors. *Geophysical Prospecting*, 58(2), 279-295.

Rawnsley, K. D., Rives, T., Petit, J. P., Hencher, S. R., & Lumsden, A. C. (1992). Joint development in perturbed stress fields near faults. *Journal of Structural Geology*, 14(8-9), 939-951.

Rotevatn, A., & Bastesen, E. (2014). Fault linkage and damage zone architecture in tight carbonate rocks in the Suez Rift (Egypt): implications for permeability structure along segmented normal faults. *Geological Society, London, Special Publications*, 374(1), 79-95.

Salah, M. G., & Alsharhan, A. S. (1998). The Precambrian basement: a major reservoir in the rifted basin, Gulf of Suez. *Journal of Petroleum Science and Engineering*, 19(3-4), 201-222.

Salomão, M. C., Marçon, D. R., Rosa, M. B., de Salles Pessoa, T. C., & Capeleiro Pinto, A. C. (2015). Broad Strategy to Face with Complex Reservoirs: Expressive Results of Production in Pre-Salt Area, Offshore Brasil. *Offshore Technology Conference*. doi:10.4043/25712-MS.

Sammis, C. G., An, L., & Ershaghi, I. (1992). Determining the 3-D fracture structure in the Geysers geothermal reservoir (No. SGP-TR-141-13). University of Southern California, Los Angeles, CA.

Sanderson, D. J., & Nixon, C. W. (2015). The use of topology in fracture network characterization. *Journal of Structural Geology*, 72, 55-66.

Sanderson, D. J., & Nixon, C. W. (2018). Topology, connectivity and percolation in fracture networks. *Journal of Structural Geology*, 115, 167-177.

1105 Schill, E., Genter, A., Cuenot, N., & Kohl, T. (2017). Hydraulic performance history at the  
 1106 Soultz EGS reservoirs from stimulation and long-term circulation tests. *Geothermics*, 70,  
 1107 110-124.

1108

1109 Schöpfer, M. P., Arslan, A., Walsh, J. J., & Childs, C. (2011). Reconciliation of contrasting  
 1110 theories for fracture spacing in layered rocks. *Journal of Structural Geology*, 33(4), 551-565.

1111

1112 Segall, P., Pollard, D.D., 1983. Joint formation in granitic rocks of the Sierra Nevada.  
 1113 *Geological Society of America Bulletin* 94, 563-575.

1114

1115 Shackleton, J. R., Cooke, M. L., Vergés, J., & Simó, T. (2011). Temporal constraints on  
 1116 fracturing associated with fault-related folding at Sant Corneli anticline, Spanish  
 1117 Pyrenees. *Journal of Structural Geology*, 33(1), 5-19.

1118

1119

1120 Sharp, I., Gillespie, P., Morsalnezhad, D., Taberner, C., Karpuz, R., Vergés, J., Horbury, A.,  
 1121 Pickard, N., Garland, J. & Hunt, D. (2010). Stratigraphic architecture and fracture-controlled  
 1122 dolomitization of the Cretaceous Khami and Bangestan groups: an outcrop case study,  
 1123 Zagros Mountains, Iran. *Geological Society, London, Special Publications*, 329(1), 343-396.

1124

1125

1126 Sibson, R. H. (1996). Structural permeability of fluid-driven fault-fracture meshes. *Journal of*  
 1127 *Structural Geology*, 18(8), 1031-1042.

1128

1129 Smith Jr, L. B., & Davies, G. R. (2006). Structurally controlled hydrothermal alteration of  
 1130 carbonate reservoirs: Introduction. *AAPG Bulletin*, 90(11), 1635-1640.

1131

1132 Solum, J. G., & Huisman, B. A. H. (2017). Toward the creation of models to predict static and  
 1133 dynamic fault-seal potential in carbonates. *Petroleum Geoscience*, 23 (1), 70-91.

1134

1135 Spina, V., Borgomano, J., Nely, G., Shchukina, N., Irving, A., Neumann, C., & Neillo, V. (2015).  
 1136 Characterization of the Devonian Kharyaga carbonate platform (Russia): Integrated and  
 1137 multiscale approach. *AAPG Bulletin*, 99(9), 1771-1799.

1138

1139 Stewart, S.A. & Podolski, R. 1998. Curvature analysis of gridded geological surfaces. In:  
 1140 Coward, M.P., Daltaban, T.S. & Johnson, H. (eds) *Structural Geology in Reservoir*  
 1141 *Characterization*. Geological Society, London, Special Publications, 127, 133–147,  
 1142 <https://doi.org/10.1144/GSL.SP.1998.127.01.11>

1143

1144

1145 Strijker, G., Bertotti, G., & Luthi, S. M. (2012). Multi-scale fracture network analysis from an  
 1146 outcrop analogue: A case study from the Cambro-Ordovician clastic succession in Petra,  
 1147 Jordan. *Marine and Petroleum Geology*, 38(1), 104-116.

1148  
1149 Tavani, S., Corradetti, A., Sabbatino, M., Morsalnejad, D., & Mazzoli, S. (2018). The Meso-  
1150 Cenozoic fracture pattern of the Lurestan region, Iran: The role of rifting, convergence, and  
1151 differential compaction in the development of pre-orogenic oblique fractures in the Zagros  
1152 Belt. *Tectonophysics*, 749, 104-119.  
1153  
1154 Tjetland, G., Kristiansen, T. G., & Buer, K. (2007, January). Reservoir management aspects of  
1155 early waterflood response after 25 years of depletion in the Valhall field. In *International*  
1156 *Petroleum Technology Conference*. International Petroleum Technology Conference.  
1157 doi:10.2523/IPTC-11276-MS  
1158  
1159 Trice, R., Hiorth, C., & Holdsworth, R. (2019). Fractured basement play development on the  
1160 UK and Norwegian rifted margins. *Geological Society, London, Special Publications*, 495,  
1161 SP495-2018.  
1162  
1163 van Golf-Racht, T. D. (1982). *Fundamentals of fractured reservoir engineering*. Elsevier.  
1164  
1165 Vidal, J., & Genter, A. (2018). Overview of naturally permeable fractured reservoirs in the  
1166 central and southern Upper Rhine Graben: Insights from geothermal wells. *Geothermics*, 74,  
1167 57-73.  
1168  
1169 Vollgger, S. A., & Cruden, A. R. (2016). Mapping folds and fractures in basement and cover  
1170 rocks using UAV photogrammetry, Cape Liptrap and Cape Paterson, Victoria,  
1171 Australia. *Journal of Structural Geology*, 85, 168-187.  
1172  
1173 Walker, R.J., Holdsworth, R.E., Imber, J., Faulkner, D.R. & Armitage, P.J. 2013. Fault zone  
1174 architecture and fluid flow in interlayered basaltic volcanoclastic crystalline sequences.  
1175 *Journal of Structural Geology*, 51, 92-104, doi: 10.1016/j.jsg.2013.03.004  
1176  
1177 Wennberg, O. P., Rennan, L., & Basquet, R. (2009). Computed tomography scan imaging of  
1178 natural open fractures in a porous rock; geometry and fluid flow. *Geophysical*  
1179 *Prospecting*, 57(2), 239-249.  
1180  
1181 Wennberg, O. P., Casini, G., Jahanpanah, A., Lapponi, F., Ineson, J., Wall, B. G., & Gillespie, P.  
1182 (2013). Deformation bands in chalk, examples from the Shetland Group of the Oseberg  
1183 Field, North Sea, Norway. *Journal of Structural Geology*, 56, 103-117.  
1184

1185 Wennberg, O. P., Casini, G., Jonoud, S., & Peacock, D. C. (2016). The characteristics of open  
1186 fractures in carbonate reservoirs and their impact on fluid flow: a discussion. *Petroleum*  
1187 *Geoscience* 22, 91-104.

1188

1189 White, W. B. (2016). Science of caves and karst: A half century of progress. *Geological*  
1190 *Society of America Special Papers*, 516, 19-33.

1191

1192 Witte, J., Bonora, M., Carbone, C., & Oncken, O. (2012). Fracture evolution in oil-producing  
1193 sills of the Rio Grande Valley, northern Neuquén Basin, Argentina. *AAPG bulletin*, 96(7),  
1194 1253-1277.

1195

1196 Woodcock, N. H., Dickson, J. A. D., & Tarasewicz, J. P. T. (2007). Transient permeability and  
1197 reseal hardening in fault zones: evidence from dilation breccia textures. *Geological Society,*  
1198 *London, Special Publications*, 270(1), 43-53.

1199

1200 Wu, X., Liang, L., Shi, Y., & Fomel, S. (2019). FaultSeg3D: Using synthetic data sets to train an  
1201 end-to-end convolutional neural network for 3D seismic fault  
1202 segmentation. *Geophysics*, 84(3), IM35-IM45.

1203

1204 Yielding, G., Needham, T., & Jones, H. (1996). Sampling of fault populations using sub-  
1205 surface data: a review. *Journal of Structural Geology*, 18(2-3), 135-146.

1206

1207 Younes, A. I., Engelder, T., & Bosworth, W. (1998). Fracture distribution in faulted basement  
1208 blocks: Gulf of Suez, Egypt. *Geological Society, London, Special Publications*, 127(1), 167-190.

1209

1210 Zahm, C. K., & Hennings, P. H. (2009). Complex fracture development related to  
1211 stratigraphic architecture: Challenges for structural deformation prediction, Tensleep  
1212 Sandstone at the Alcova anticline, Wyoming. *AAPG bulletin*, 93(11), 1427-1446.

1213



## Figures

Figure 1. Summary of global frequency of fractured reservoirs according to lithology and tectonic setting at the time of trap formation. From C&C Reservoirs (2020).

Figure 2. End member fracture systems showing an organized and well-connected system of stratabound joints and non-stratabound fractures that are strongly clustered.

Figure 3. a) Stratabound joints developed limestones within a limestone/marl sequence from the Lias (Early Jurassic) at Lavernock Point, Wales. Joints are more narrowly spaced in the thinner units than in the lower, composite unit. The fracture aperture has been greatly enlarged by recent dissolution to form karst fissures. Ruler extended to 1 m. b) Clustered non-stratabound joints developed in Silurian granodiorite from Rolfsnes, western Norway. Cliff height ca 4 m.

Figure 4. Example of a conceptual model of fracturing in an extensional setting showing faults and joints and their relationship to stratigraphy (after Gross and Eyal 2007).

Figure 5. Normal fault in Cretaceous platform limestone from Maiella, Italy. The fault has a displacement of about 50 m. The brecciated fault core occurs within a lozenge and the surrounding rock is fractured, forming a damage zone. Alun Williams for scale.

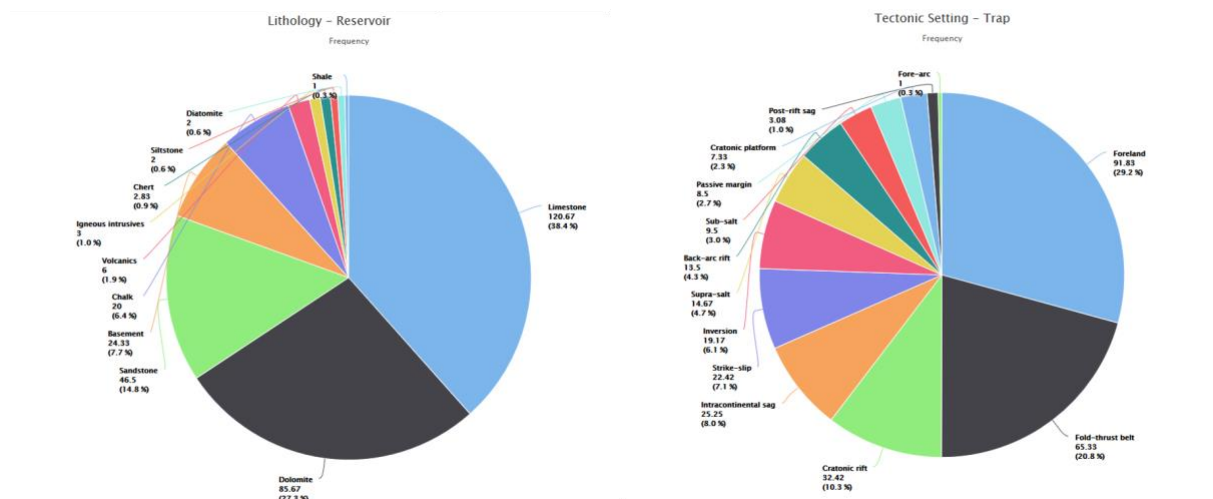
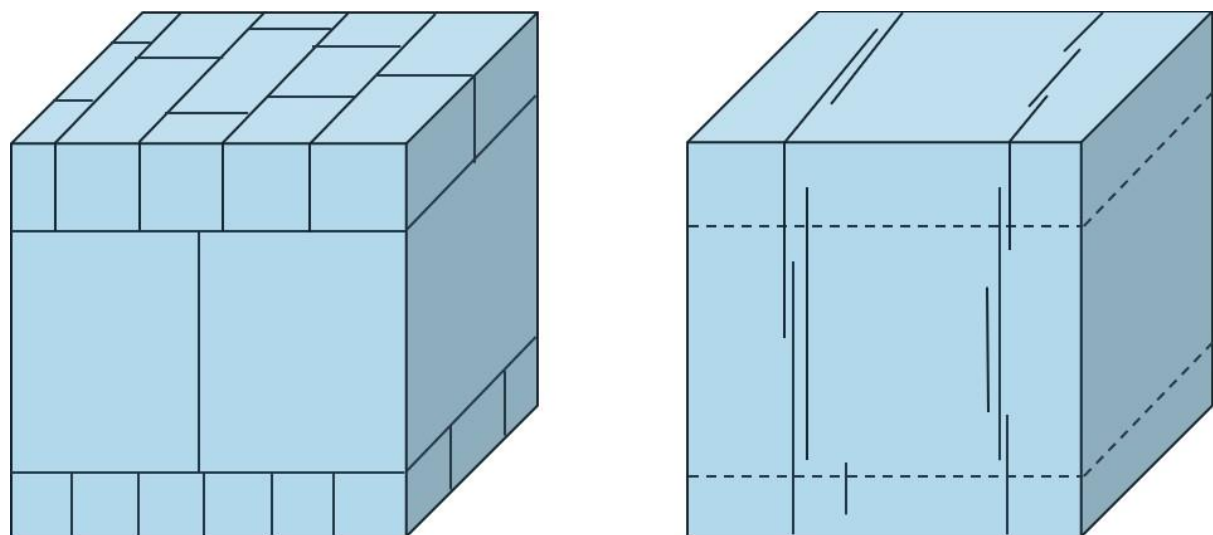


Figure 1



Stratabound

Non-stratabound

Figure 2



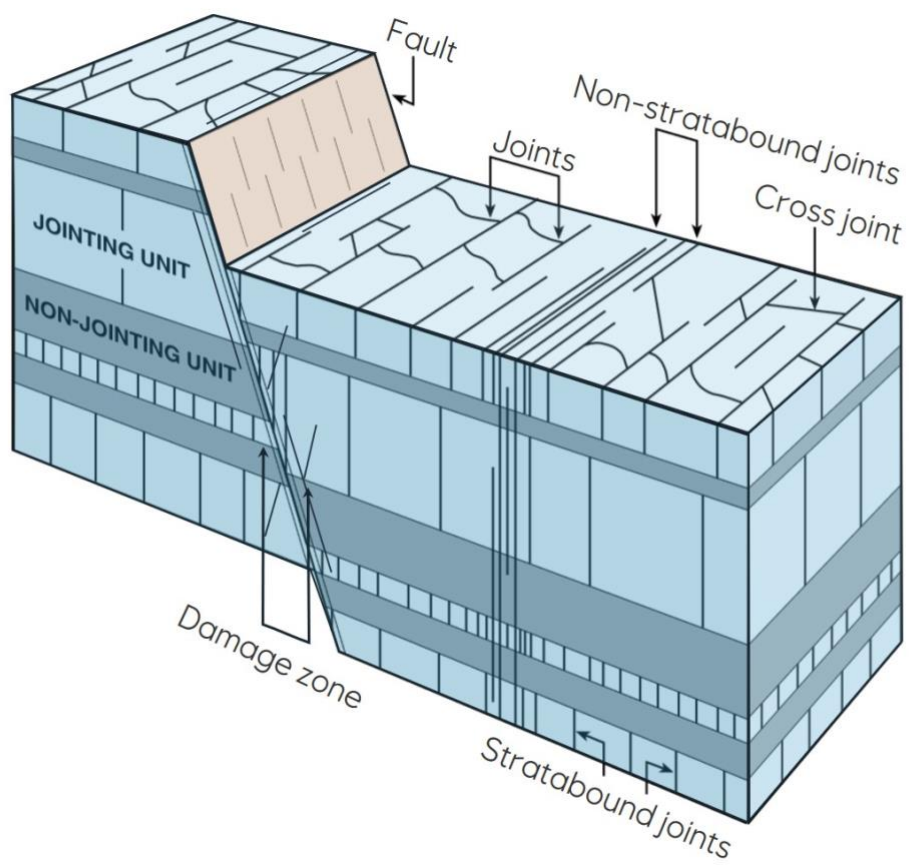
1256



1257

1258    Figure 3a and b





1259  
1260 Figure 4



1261

1262 Figure 5

1263